Contents lists available at ScienceDirect

Chemical Engineering Journal

journal homepage: www.elsevier.com/locate/cej

Study of a multitubular fixed-bed reactor for ethylene production via ethane oxidative dehydrogenation

Eduardo López [a,c,*], Eleni Heracleous [b], Angeliki A. Lemonidou [b], Daniel O. Borio [a]

[a] Planta Piloto de Ingeniería Química (UNS-CONICET), Camino La Carrindanga km. 7, 8000 Bahía Blanca, Argentina
[b] Department of Chemical Engineering, Aristotle University of Thessaloniki and Chemical Process Engineering Research Institute (CERTH/CPERI),
P.O. Box 1517, University Campus, GR-54006 Thessaloniki, Greece
[c] Institut de Tècniques Energètiques, Universitat Politècnica de Catalunya, Diagonal 647, ed. ETSEIB, 08028 Barcelona, Spain

A R T I C L E   I N F O

A B S T R A C T

In the present contribution, a theoretical study of a multitubular fixed bed reactor for the ethane to ethylene oxidative dehydrogenation reaction over a highly active and selective Ni–Nb–O mixed oxide catalyst is presented. Two reactor designs are proposed and their performance is analyzed by means of a mathematical model of the catalytic bed.

The results suggest that the reactor operation would be feasible, provided that high heat transfer area per unit volume and low oxygen concentrations along the tube are maintained. A two-bed multitubular reactor with intermediate air injection proved to be superior to a single-bed design. In fact, the two-bed configuration offers higher ethylene production rates, due to the increased ethylene selectivity while operation under lower oxygen partial pressures.

© 2008 Elsevier B.V. All rights reserved.

1. Introduction

Industrial ethylene production is nowadays mainly performed by thermal steam cracking (pyrolysis) of naphtha or ethane. This process is highly endothermic and requires elevated amounts of energy. The most promising alternative to the conventional process is the ethane oxidative dehydrogenation (ODH) to ethylene, in the presence of a suitable catalyst [1]. The ODH reaction proceeds via a triangular series/parallel reaction scheme with the undesired complete combustions of both ethane and ethylene. The reactions are irreversible and exothermic; therefore, no external heating is required and no equilibrium limitations are observed. The system of reactions is represented by

$$C_2H_6 + \frac{1}{2}O_2 \rightarrow C_2H_4 + H_2O \tag{1}$$

$$C_2H_6 + \frac{7}{2}O_2 \rightarrow 2\,CO_2 + 3\,H_2O \tag{2}$$

$$C_2H_4 + 3\,O_2 \rightarrow 2\,CO_2 + 2\,H_2O \tag{3}$$

Ethane oxidative dehydrogenation has been studied over a wide range of catalytic materials mostly based on reducible metal oxides

[2–7]. Many of them present the required activity; however, the majority exhibits low selectivity to the desired reaction at high conversion levels (Eq. (1)). In a recent publication, Heracleous and Lemonidou [8,9] reported the high potential of a new class of catalytic materials based on nickel for the oxidative dehydrogenation of ethane to ethylene. The developed bulk Ni–Nb–O mixed nano-oxides exhibit both high activity at low reaction temperature and very high selectivity, resulting in an overall ethene yield of 46% at 400 °C. Detailed characterization of the nano-oxides on a microscopic level linked the excellent catalytic behaviour to the electronic and structural rearrangement induced by the incorporation of niobium cations in the NiO lattice. Considerable work on the macroscopic level led to the development of a detailed kinetic model, describing the catalytic behavior in a wide range of operational parameters.

As mentioned elsewhere [10–12], for such exothermic processes, the control of the reaction temperature appears as a key factor to maintain a good selectivity level; the generated heat has to be efficiently removed from the catalyst bed. Therefore, the reactor choice and its design acquire an outstanding importance.

Multitubular reactors are commonly used in industry to carry out exothermic processes. Up to 30 000 tubes of small diameter are employed in order to minimize thermal radial gradients and enhance the ratio between the heat-exchange area and the reaction volume. The bundle of tubes is immersed in a shell through where a proper coolant flows [10].

---

* Corresponding author at: Institut de Tècniques Energètiques, Universitat Politècnica de Catalunya, Diagonal 647, ed. ETSEIB, 08028 Barcelona, Spain. Tel.: +34 93 4137498; fax: +34 93 4017149.
E-mail address: e.lopez@upc.edu (E. López).

Nomenclature

A_T	tube cross-section, m²
c_p	specific heat, kJ/(mol K)
d_p	particle equivalent diameter, m
d_t	tube diameter (internal), m
E	activation energy, J/mol
f	friction factor
F	molar flowrate, kmol/s
k_R	reaction rate constant at reference conditions ($T_R = 543$ K), kmol/kg$_{cat}$/s/Pa^{a+b}
L	tube length, m
m	mass flowrate, kg/s
n_{BF}	number of baffles
n_t	number of tubes
P	pressure, atm
r	reaction rate, mol/(kg$_{cat}$ s)
R	universal gas constant = 8.314 J/(mol K)
S_G, S_I	global and instantaneous selectivity, respectively (see Eqs. (10) and (11))
T	temperature, °C (K for kinetic expression, Eq. (9))
T_R	reference temperature for kinetic expression (Eq. (9)), K
u_s	superficial velocity, m/s
U	overall heat-transfer coefficient, kJ/(s m² K)
x	conversion
y	molar fraction
z	axial coordinate, m

Subindex

0	inlet conditions
air	intermediate air stream, Design II
c	coolant
cat	catalyst
g	process gas
HC	hydrocarbon
i	reaction number (Eqs. (1)–(3))
inert	filled with inert particles
j	component number (six components)
L	at bed exit
max	maximum value
z	at specific axial coordinate

Superindex

1	corresponding to bed 1
2	corresponding to bed 2
5 atm	at 5 atm of inlet pressure
10 atm	at 10 atm of inlet pressure
a_i	reaction order with respect to hydrocarbon
b_i	reaction order with respect to oxygen

Greek letters

ΔH	heat of reaction, kJ/mol
ΔP	pressure drop, atm/m
ε	bed void fraction, $(1 - m_{cat}^3)/m_{bed}^3$
$\theta_p, \theta_{p,max}$	parametric sensitivity, maximum axial value (see Eq. (12))
ν_{ji}	stoichiometric coefficient of component j in reaction i
ρ_B	bed density, kg$_{active\,cat}$/m$_{bed}^3$

Although, as aforementioned, ethane oxidative dehydrogenation has been studied widely over a wide range of catalytic materials, there seems to be a lack of research on the engineering aspects of the reaction for industrial implementation under realistic reactor configuration and conditions. The majority of relevant publications in literature refer to the oxidative dehydrogenation of higher alkanes, such as propane and butane [13,14], while publications on ethane are, to our best knowledge, scarce [15].

In the present contribution, a theoretical study of a multitubular fixed bed reactor for the ethane to ethylene oxidative dehydrogenation reaction over a Ni–Nb–O mixed oxide catalyst is presented. The performance of the ODH reactor is analyzed by means of a mathematical model of the catalytic unit. The influence of several operational and design variables, such as pressure, temperature, coolant flowrate and catalyst geometry is discussed. An alternative design comprising two catalytic beds in series with distributed oxygen injection is presented to analyze the effect of the oxygen-feed mode.

2. Mathematical model and reactor design considerations

A one-dimensional, pseudo-homogeneous, steady-state model has been used to represent the ODH of ethane to ethylene in a wall-cooled multitubular fixed-bed reactor. A first section of the tubes was considered filled with inert particles, with the rest of the tubes filled with the Ni–Nb–O oxydehydrogenation catalyst. The coolant was assumed to flow in the shell co-currently with the process gas. By this configuration, the low-temperature incoming process gas (mixture of ethane and air) is preheated up to the reaction temperature at the expense of the coolant with enters the shell at higher temperature. Inert particles are selected for the inlet section instead of expensive catalyst particles as gas temperatures are too low there to give appreciable reaction rates. Based on the operation with high total flowrates through the packed bed and the use of tubes of small diameter (1″), axial mass and energy dispersions were assumed to be negligible. The use of such low-diameter tubes and high flowrates supports the assumption of 1D model avoiding the occurrence of radial temperature profiles and assuring good radial mixing (plug flow). Internal and external mass and energy transport limitations were also not considered based on the use of a washcoat with low thickness and high flowrates, respectively. The reactor shell was assumed adiabatic. In addition to mass and energy balances, the continuity equation was included in the model to predict the pressure drop in the reactor. The friction factor f proposed by Ergun was adopted [16]. The balances used to represent the steady-state reactor behavior, along with the corresponding initial conditions, are presented below.

Mass balances, process gas:

$$\frac{dF_j}{dz} = n_t A_T \rho_B \sum_{i=1}^{3} \nu_{ij} r_i, \quad j = 1, \ldots, 6 \tag{4}$$

Energy balance, process gas:

$$\frac{dT_g}{dz} = \frac{n_t A_T \rho_B \sum_{i=1}^{3} r_i(-\Delta H_i) - n_t A_T (4/d_t) U(T_g - T_c)}{\sum_{j=1}^{6} F_j c_{p_j}} \tag{5}$$

Energy balance, coolant: $\quad \dfrac{dT_c}{dz} = \dfrac{n_t \pi d_t U(T_g - T_c)}{m_c c_{p_c}} \tag{6}$

Table 1
Kinetic parameters for reaction rate expressions, Eq. (9) [9]

Reaction (i)	$k_{R,i}$ (kmol/kg$_{cat}$/s/Pa^{a+b})	E_i (J/mol)	a_i	b_i
1	4.177×10^{-10}	96 180	0.520	0.213
2	1.272×10^{-13}	76 210	0.547	0.829
3	9.367×10^{-11}	98 420	0.475	0.319

Pressure drop, process gas :

$$\frac{dP}{dz} = -f \frac{\rho_g u_s^2}{d_p} \tag{7}$$

Initial conditions :

$$\text{At } z = 0 \quad F_j = F_{j,0}, \quad T_g = T_{g,0}, \quad T_c = T_{c,0}, \quad P = P_0 \tag{8}$$

A Ni–Nb–O mixed-oxide catalyst ($Ni_{0.85}Nb_{0.15}$) was used for the oxidative dehydrogenation of ethane to ethylene, as reported by Heracleous and Lemonidou [8,9]. A power-law-type expression as shown by Eq. (9) was considered to model the reaction rates for reactions (1)–(3) (used in Eqs. (4) and (5)). The ideal gas assumption is considered to calculate the partial pressures from the correspondent molar flows. Table 1 reports the corresponding parameters for r_i ($T_R = 543$ K, p_j in Pa) [9].

$$r_i = k_{R,i} \ e^{-(E_i/R)(1/T - 1/T_R)} p_{HC_i}^{a_i} p_{O_2}^{b_i} \tag{9}$$

The catalyst particles were assumed to be 6 mm diameter spheres, of the *egg-shell*-type. The washcoat covering the spheres, where the active components are impregnated, was assumed to have a mean thickness of 70 μm. A bulk void fraction of $\varepsilon = 0.38$ is consequent with the modeled catalyst particles [16]. The use of washcoated particles results in a low bed density of $\rho_B = 50$ kg$_{cat}$/m^3, favoring the moderation of the heat generation rate per unit volume and, consequently, achieving milder operating conditions. Additionally, and in order to analyze the influence of the catalyst geometry on the pressure drop, hollow cylinders (*Raschig-ring* type) of 6 mm × 6 mm × 2 mm were also modeled. In this scenario, a bed void fraction of 0.48 was calculated, in agreement with literature [17]. By adjusting the washcoat thickness of the hollow cylinders (mean thickness of washcoat in Raschig-rigs of 60 μm) to compensate the increase in surface area, the above specified value for the bed density of $\rho_B = 50$ kg$_{cat}$/m^3 was kept constant.

The guidelines suggested in Froment and Bischoff [16] were adopted for the evaluation of the overall-heat-transfer coefficient (U), where the value of the heat-transfer coefficient for the process gas side was calculated by means of the equation of Calderbank and Pogorski [18] and that corresponding to the coolant side by using a correlation reported by Kern [19]. Molten salts were selected as coolant (properties taken from [11]), based on their stability at the operating temperature level of ∼400 °C. Co-current flow operation was assumed for the molten salts to avoid steady-state multiplicity associated with heat feed-back and to obtain lower temperature excursions, as reported elsewhere [12]. Baffles were considered

placed in the shell to assure appropriate heat transfer coefficients on the coolant side.

The global selectivity (S_G) is calculated as the ratio between the amount of ethylene produced and the amount of ethane consumed, from the reactor inlet up to the desired axial coordinate. This integral variable is of key importance in the ethane ODH process, as it determines the global yield of the plant. The instantaneous selectivity (S_I), defined as the quotient of the local net ethylene production rate and the net ethane consumption rate, represents the selectivity pattern in a particular axial coordinate of the reactor. It is directly related to the local operating conditions (concentrations, temperature, pressure) and independent of the up-stream history. Both selectivities (global and instantaneous, respectively) are calculated using the following equations:

$$S_G = \frac{F_{C_2H_4,z} - F_{C_2H_4,0}}{F_{C_2H_6,0} - F_{C_2H_6,z}} \tag{10}$$

$$S_I = \frac{r_1 - r_3}{r_1 + r_2} \tag{11}$$

To simulate an industrial scale operation, a production of at least 100 000 ton/year of ethylene was set. Furthermore, a maximum allowable pressure drop of 0.3 atm/m was assumed to avoid catalyst attrition and to provide enough robustness in case of moderate plugging [20,11]. Therefore, two reactors in parallel are required to satisfy both production rate and pressure drop constraints, each with 10 000 tubes of 1″ nominal diameter. The shell diameter was calculated following the guidelines provided by Rose [11].

Different scenarios regarding the feed composition can be proposed for the ethane-ODH process [10]. In the present contribution, the feed is comprised of a large excess of ethane with a small amount of air. This appears to be the simplest case as no air separation is required to feed pure oxygen to the reactor, which would result at first glance in higher investment costs. Unconverted ethane, after separation from the other educts from the reactor, has to be recycled to the reactor inlet. In addition, the reaction mixture is out of the flammability limits. At any oxygen partial pressure lower than the maximum one assumed for this working hypothesis, safe operation out of the flammability limits is assured. A possible drawback of this scenario could be the not-straightforward separation of the produced ethylene and the over sizing of the equipment due to the nitrogen injected with the reaction air. The selected operating conditions lead always to complete oxygen conversion in the catalytic bed.

Low inlet pressure values of around 5 atm are proposed to increase somehow the gas density and avoid prohibitive pressure drops. This pressure level introduces another advantage: the internal heat-transfer coefficient and, consequently, the value of U increases [21]. Operation at higher pressures is not recommended as ethylene selectivity deteriorates [9].

Alternatively to the proposed single-bed reactor design (Design I), a two-bed multitubular reactor with intermediate air injection
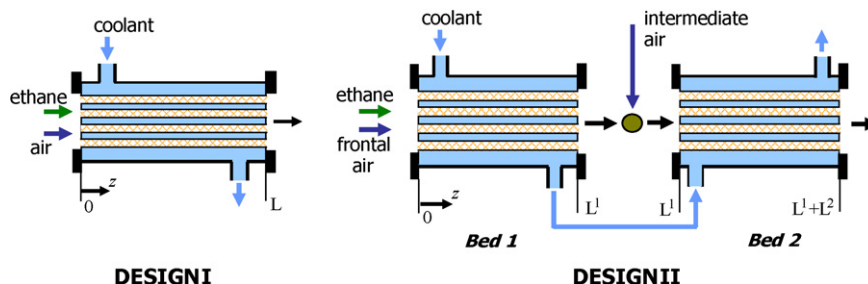

Fig. 1. Schematic representation of the modeled multitubular reactors.
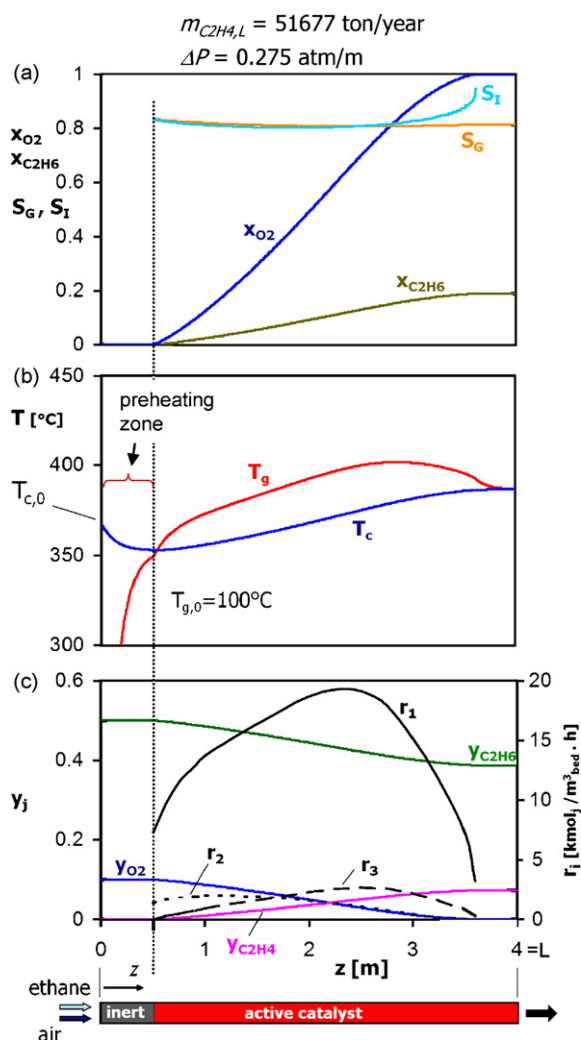
Fig. 2. Axial profiles for simulations of reference case (see Table 2), Design I. (a) Ethane and oxygen conversions, global and instantaneous selectivities, (b) process gas and coolant temperatures, and (c) ethane, oxygen and ethylene molar fractions, reaction rates.

(Design II) is also studied to analyze the operation under lower oxygen partial pressures to improve selectivity. Fig. 1 shows schematic representations of the proposed designs.

3. Results and discussion

In Fig. 2a, ethane and oxygen conversions ($x_{C_2H_6}$ and x_{O_2}) and both global and instantaneous selectivities (S_G and S_I, respectively) are shown for a multitubular reactor with front air injection (Design I). For this reference case, the main operative conditions and design parameters are reported in Table 2. As observed, the achieved ethane conversion is low ($\sim$19%) because of the high excess of ethane. This may cause inconvenience to the separa-

Table 2
Operative conditions and design parameters for single-bed reactor simulations (Design I)

$y_{O_2,0}$	0.1	$F_{g,0}$	0.8333 kmol/s	L_{inert}	0.5 m
$y_{N_2,0}$	0.4	$T_{g,0}$	100 °C	d_t	0.0266 m
$y_{C_2H_6,0}$	0.5	P_0	5 atm	n_t	10 000
$y_{CO_2,0}$	0	$T_{c,0}$	367.5 °C	ρ_B	50 kg$_{active\ cat}$/m$^3_{bed}$
$y_{H_2O,0}$	0	m_c	300 kg/s	n_{BF}	3
$y_{C_2H_4,0}$	0	L	4 m	d_P	0.006 m

tion units downstream the reactor due to the low ethylene/ethane ratios. In addition, high ethane recycle flowrates are required. An oxygen inlet molar fraction of 10% represents the maximum oxygen content for this system. Higher oxygen amounts would lead to a selectivity drop and generation of a pronounced hot spot. In addition, the resulting reaction mixtures would be closer to the flammability limits. The desired ethylene production rate of 50000ton$_{C_2H_4}$/reactor/year is achieved via this design without violating the maximum allowable pressure drop, as also indicated in Fig. 2a.

The corresponding axial temperature profiles for the process gas (T_g) and the coolant (T_c) are presented in Fig. 2b. A smooth axial T_g profile in the active catalyst zone is observed, with a maximum value of 402 °C. The first 0.5 m of the reactor, where the inert particles are disposed, acts efficiently as preheater increasing the gas temperature from 100 °C to the reaction temperature of $\sim$350 °C. The coolant temperature drops in the preheating region, followed by an increase in the reaction zone up to 20 °C higher than the inlet value. A relatively low coolant mass flowrate relative to the heat evolved in the reaction is used, achieving a descend in the maximum temperature of the process gas ("co-current effect"). The necessary linear velocity of the coolant across the tube bundle to get proper external heat transfer coefficients is assured through the use of baffles in the shell [12]. It was also observed that the reactor performance strongly depends on the value of the overall heat-transfer coefficient (U). Therefore, its correct prediction proves to be a key issue in this system.

Both global and instantaneous selectivities (Fig. 2a) show a slight decrease with the axial coordinate due to the temperature increase from 350 to around 400 °C in the first 2/3 of the active zone of the catalyst bed. The adjusted activation energies point out that an intermediate temperature level of around 350 °C favors the desired oxydehydrogenation reaction (Eq. (1)) [9]. Lower temperatures deteriorate the selectivity enhancing ethane complete combustion (Eq. (2)), while higher temperatures favor the ethylene complete combustion (Eq. (3)). In the final zone of the catalytic bed the oxygen depletion leads to an increase in the selectivities (in particular, S_I in the region where $x_{O_2} \to 1$). Indeed, as reported by Heracleous and Lemonidou [9], the reaction orders with respect to oxygen for reactions (1)–(3), show that reaction 1 is favored by lower oxygen concentrations (see Table 1). For the simulated conditions, a very good global selectivity level is calculated for the entire reactor, with an outlet S_G of around 0.81 (see Fig. 2a). As complete recycle of unconverted ethane is assumed, the reactor global selectivity is equal to the plant yield, and, consequently, the amount of fresh ethane to be fed is determined. For this simulation scenario, with a production of 51 677 ton/reactor/year of ethylene and a plant yield of 0.81, a fresh ethane feed of 68 355 ton/reactor/year is required.

Axial profiles for the reaction rates and the molar fractions of oxygen, ethane and ethylene are presented in Fig. 2c. These profiles agree well with the calculated values for S; reaction (1) shows much higher rates than the other reactions. An additional design requirement for the ODH-reactor is to achieve complete oxygen conversion at an axial coordinate close to the reactor end. An early oxygen depletion has been reported to favor deactivation on most catalytic systems [22]; conversely, the achievement of a non-complete oxygen conversion scenario would not be convenient due to problems in the separation units downstream the reactor and the coexistence of oxygen and ethane in the recycle stream.

3.1. Effect of feed inlet pressure

Simulation of the ethane ODH single-bed reactor was also performed at higher inlet pressures than the one reported for the
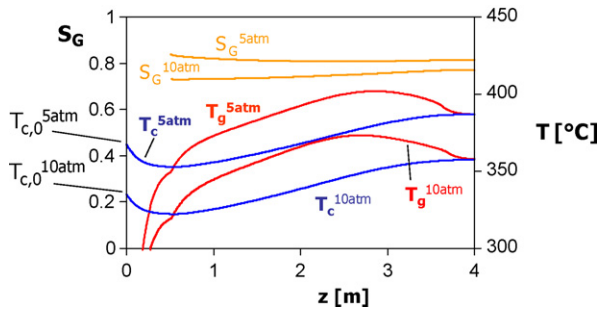
Fig. 3. Global selectivity and process gas and coolant temperatures axial profiles for inlet pressures of 5 atm (reference case) and 10 atm. Design I, other conditions as in Table 2.

Fig. 4. ♦ Effect of the coolant mass-flowrate on the inlet temperature of the coolant required to reach complete oxygen conversion on the axial coordinate as presented in Fig. 2a. ▲ maximum axial sensitivity of the reactor (see Eq. (12)) as function of the coolant flowrate. Design I, other conditions as in Table 2.

reference case (P_0 = 5 atm, see Table 2), in order to analyze the influence of this variable on the reactor performance. Fig. 3 presents a comparison of the gas and coolant temperatures and the global selectivities for inlet pressures of 5 and 10 atm. Higher operation pressures accelerate the reaction rates as a consequence of the increase in the reactants partial pressures. Therefore, lower inlet coolant temperatures are required (in this case, $T_{c,0}$ = 335 °C) to moderate the heat generation rate and achieve smooth temperature profiles; operation with $T_{c,0}$ = 367.5 °C (as in Table 2) leads to a pronounced hot spot (maximum $T_g \sim 650$ °C). Both global and instantaneous selectivities deteriorate with the increase in pressure; an outlet value for S_G of 0.77 leads to an ethylene production of around 43 400 ton/year (84% of the reference case). The origin of this decrease in ethylene selectivity at higher operating pressures could be traced back to the kinetic parameters of the reaction rate expressions. As shown in Table 1, the primary oxidation of ethane to CO_2 has a much higher oxygen reaction order (0.829) than the other two reactions. Ethane reaction order on the other hand is comparable for all three reactions. Therefore, the pressure increase favours the total oxidation reaction and leads to the observed increase in the CO_2 selectivity at the expense of ethylene production. A reduction of the pressure drop from 0.275 atm/m for P_0 = 5 atm to 0.119 atm/m for P_0 = 10 atm is calculated as a consequence of the increase in the gas density. Although higher values of inlet (and operating) pressure reduce the pressure drop and increase the value of the overall heat-transfer coefficient (U), the operation at the lower allowable inlet pressure (observing the maximum allowable pressure drop constraint of 0.3 atm/m) is recommended as the increase in selectivity maximizes the reactor ethylene productivity.

3.2. Effect of coolant flowrate and coolant inlet temperature

In this kind of processes, where high thermal effects are involved and the performance of the reactor is greatly influenced by the ability to remove the produced heat and control the reaction temperature, the coolant flowrate and its temperature level represent key variables of outstanding importance. Fig. 4 depicts graphically the influence of these variables on the reactor performance. The coolant inlet temperature and the reactor sensitivity towards changes on $T_{c,0}$ are plotted against the reciprocal of the coolant mass flowrate, in order to reach total oxygen conversion at the same axial coordinate as reported in Figs. 2 and 3 and using the design parameters and operating conditions already presented in Table 2. The lower curve, representing the variation of the coolant inlet temperature, shows a monotonous drop as the coolant flowrate decreases. As shown in Fig. 2b, after an initial drop in the inert region, the coolant recovers its formerly given heat in the catalytic region to reach higher levels than the inlet value. If the flowrate increases, the variation of its temperature along the reactor obviously decreases,
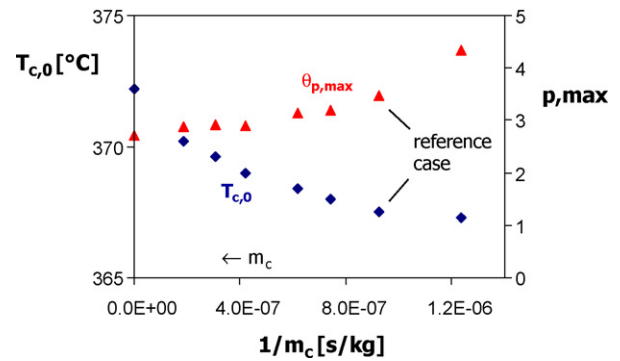
as also its mean temperature. Therefore, to reach total conversion of oxygen at the same specified axial coordinate, the coolant inlet temperature has to be increased.

The sensitivity of the reactor to changes on the coolant inlet temperature can be approximated by means of the following expression:
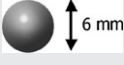
$$\theta_p = \frac{dT_g}{dT_{c,0}} \cong \frac{\Delta T_g}{\Delta T_{c,0}} \tag{12}$$

To characterize the parametric sensitivity of each operating condition, the maximum value of the axial sensitivity profile given by Eq. (12), $\theta_{p,max}$, is selected. $\theta_{p,max}$ monotonously increases with the reduction of the coolant mass flowrate (m_c) because lower m_c values lead to lower overall heat transfer coefficients. For the selected coolant mass flowrate of 300 $kg_{coolant}$/s (reference case), a sensitivity of 3.5 is observed. This value represents an appropriate compromise level: lower flows would lead to higher sensitivities and unstable reactor operation; conversely, higher coolant flowrates would be not feasible as the pumping power to move the molten salts through the shell would be excessive.

3.3. Effect of catalyst geometry

Operation with spherical washcoated pellets, although conventional, causes a considerable pressure drop for the feed flowrates required to achieve the specified rate of ethylene production. An alterative in the pellet geometry and specifically, the use of washcoated hollow cylindrical pellets (*raschig-ring* type) is analyzed in this section. The studied scenario would correspond to the case of a change of the catalyst under use, i.e., the reactor dimensions remain unaltered and the operating conditions are adjusted. Table 3 presents a comparison of the reactor performance when using the two catalyst geometries. The main dimensions for these two types are also included. The increase in the bed void fraction (ε) for the hollow cylinders induces an increase in the processed gas flowrate without violation of the pressure drop constraint. This flowrate increment leads to an increase in the ethylene production rate of 46.5% compared to the reference case. The preheating of a higher incoming feed flowrate (from its inlet temperature of 100 °C to the reaction temperature) requires, for the same coolant mass flowrate, an increase of the coolant inlet temperature. The results also demonstrate an appreciable increase of the maximum temperature of the process gas due to the higher total amount of generated heat and a higher coolant mean temperature. The pointed need of increasing the coolant inlet temperature (and, consequently, the mean gas temperature along the bed) could appear at first glance as a disadvantage when changing to a Raschig-ring catalyst geome-

Table 3
Influence of the catalyst geometry: comparison of performance (Design I)

Catalyst geometry		ε	$F_{g,0}$ (kmol/s)	$T_{c,0}$ (°C)	$T_{g,max}$ (°C)	C_2H_4 productivity (ton/year)	ΔP (atm/m)
Spheres	6 mm	0.38	0.8333	367.5	402	51 677	0.275
Hollow cylinders	2 mm 6 mm 6 mm	0.48	1.2083	379	428	75 700	0.273

try. It is due to the scenario under evaluation which requires leaving the reactor dimensions unchanged. In case that the reactor design could be adapted to the use of this potentially much convenient catalyst (i.e., changing the scenario to a "reactor design situation") then this adverse effect would be eliminated or at least strongly attenuated.

3.4. Effect of distributed oxygen feed

Noticeable improvements are achieved when a design comprising two catalyst beds in series with additional intermediate air injection is considered (Design II, see Fig. 1). The coolant is assumed to flow in series in the shells of the two beds, with the same mass flowrate as in the reference case. The total catalyst mass is maintained constant as the one reported for the previous simulations (equal number of tubes, Table 2), as also the length of the inert region in Bed 1. The results presented in the present contribution

Table 4
Operative conditions and design parameters for ODH-reactor simulations with two beds in series with intermediate air injection (Design II)

Bed 1			Bed 2		
$y_{O_2,0}$	0.0545	$F_{g,0}$	0.5729 kmol/s	F_{air}	0.2604 kmol/s
$y_{N_2,0}$	0.2182	$T_{c,0}$	375 °C	T_{air}	100 °C
$y_{C_2H_6,0}$	0.7273	n_t	10 000	n_t	10 000
$y_{CO_2,0}$	0	L	2 m	L	2 m
$y_{H_2O,0}$	0	L_{inert}	0.5 m	L_{inert}	0 m
$y_{C_2H_4,0}$	0	n_{BF}	1	n_{BF}	1

Note: other data as reported in Table 2.

correspond to a non-optimized situation where both beds have the same length and are fed with the same amount of oxygen per unit catalyst mass and a total oxygen amount equal to the reference case. More operating conditions and design parameters are reported in Table 4.
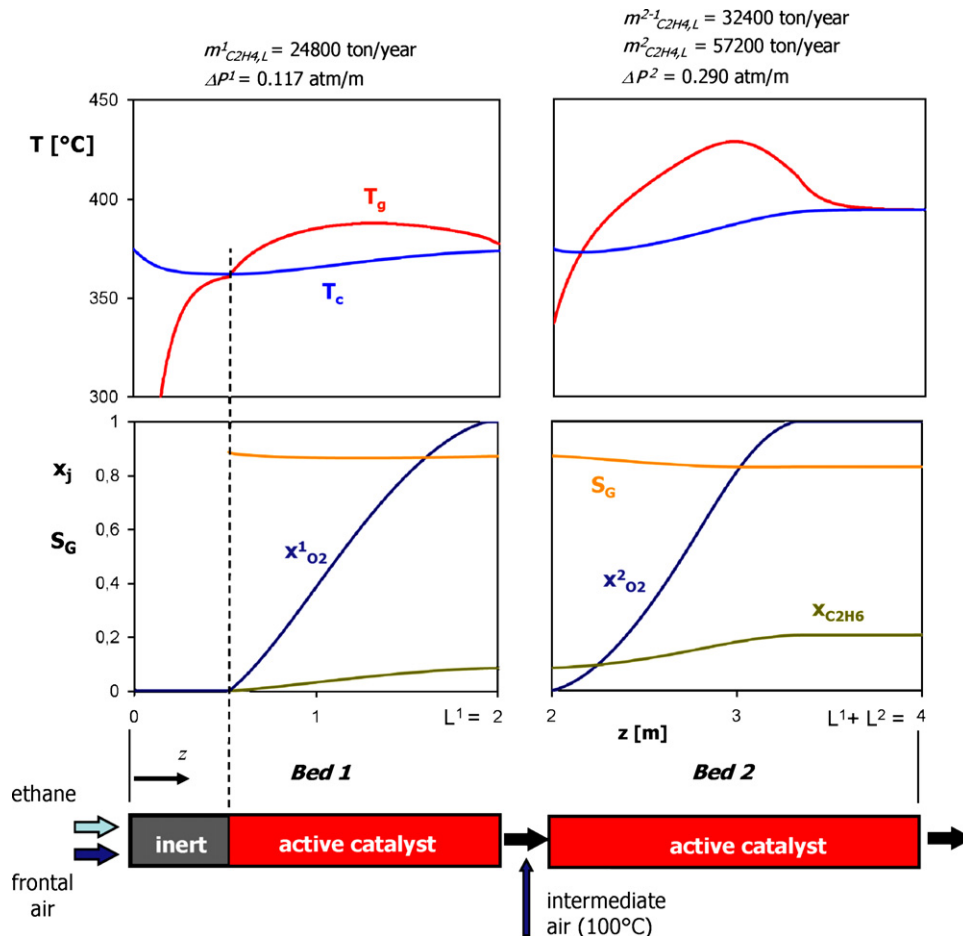

Fig. 5. Ethane and oxygen conversions, global selectivity and temperature axial profiles for Beds 1 and 2. Design II, design parameters and operating conditions as in Table 4.

Fig. 5 shows ethane and oxygen conversions, global selectivity and gas and coolant temperatures axial profiles for Design II. Ethylene productivities and pressure drops for each bed are also reported. The process gas temperature profile shows two noticeable features: a beneficial cold-shot effect in the mixing point with the colder intermediate air, and a more pronounced temperature excursion in the second bed, product of the renewed oxygen partial pressure. In both beds total oxygen conversion is reached near the bed outlet. In this two-bed scenario, it is specially important to assure total oxygen conversion in the first bed. If not, unreacted oxygen would mix with the incoming intermediate oxygen giving a too high oxygen partial pressure in the inlet of the second bed that could lead to pronounced hot spot formation and decrease of the outlet selectivity. With the introduction of Design II, with its distributed oxygen feed facility, the per-pass ethane conversion (including both beds) increases by ∼1.6% (from 18.9% for Design I to 20.5% here). Similarly, the outlet global selectivity increases from 0.81 to 0.83. The decreased mean oxygen concentration enables an increase in the fresh ethane feed to be processed of 8.3% without violating the operating constraints (maximum temperature, maximum pressure drop). In the present system a complete separation of the produced ethylene and the unconverted ethane in the outlet stream of bed 2 is assumed (recycle contains no C_2H_4; complete global C_2H_6 conversion when balanced over both beds and recycle). This assumption, added to the above reported increases of per-pass ethane conversion, outlet global selectivity and ethane fresh flowrate leads to an increase of the produced ethylene flowrate of c.a. 10.6%. Additionally, a decrease of the recycle stream flowrate is achieved.

The favourable results obtained with a distributed oxygen feed are consistent with literature data. In a similar work performed by Al-Sherehy et al. [23], where a simple model was used to simulate ethane ODH over Mo–V–Nb in a fixed-bed reactor, a 30% increase in the ethylene selectivity was observed when oxygen was distributed over 2000 injections points along the length of the reactor. It has been reported in general that the distribution of oxygen feed along the length of the reactor, either with the use of oxygen selective membranes or multiple injection, produces not only greater selectivities with respect to conventional feed arrangements, but also a safer operation with reduced formation of hot spots and a lower probability of runaway [24–26]. The avoidance of hot spots gives additional increments of selectivity by suppressing undesired reactions that take place at high temperatures and helps to extend catalyst life. The distribution of oxygen also allows a wider range of operating conditions, as it is possible to operate at overall hydrocarbon to oxygen ratios that would be within the explosive region if the same composition was fed at the entrance of a conventional fixed bed reactor, consistent with the results of the present work. An optimization of Design II regarding the relative length of each bed and the amount of oxygen fed is the subject of on-going work and is expected to provide even more auspicious results. Investigations will also be carried out to further investigate multipoint oxygen injection and the distribution of oxygen via membranes.

4. Conclusions

The feasibility of carrying out the catalytic oxidative dehydrogenation of ethane to ethylene in a large-scale multitubular reactor has been analyzed. The results suggest that the reactor operation would be feasible, provided that high heat transfer areas per unit volume and low to moderate oxygen partial pressures are maintained. *Egg-shell*-type catalysts lead to a feasible operation through the moderation of the heat generation rate. Although operation with spherical catalyst pellets is realistic, the introduction of catalyst geometries providing higher bed void fractions (e.g., hollow

cylinders) would lead to a minimization of the pressure drop and would allow the processing of higher gas flowrates, leading consequently to increased ethylene production rates. Low operation pressures, a few bars over atmospheric, should be selected resulting from a compromise between an increase in gas density to satisfy both pressure drop and productivity constraints and the drop of selectivity with the increase in pressure. The oxygen distribution along the reactor axial coordinate has a positive impact on the reactor performance due to an improvement in the selectivity based on the operation with lower oxygen partial pressures. A membrane reactor for the continuous axial feed of oxygen is currently under study for the ODH of ethane to ethylene over Ni-based mixed oxide catalysts.

Further studies should be carried out, aiming to analyze the influence of the intraparticle mass-transfer limitations and the importance of the temperature gradients along the radial coordinate. A more extensive parametric sensitivity analysis should also be performed to compare the different designs and determine the best oxygen-feed policy. These studies are currently on going and will be presented in future publications.

References

[1] G. Centi, F. Cavani, F. Trifiro, Selective Oxidation by Heterogeneous Catalysis, Kluwer Academic Publishers/Plenum Press, New York, USA, 2001.
[2] M.A. Banares, Supported metal oxide and other catalysts for ethane conversion: a review, Catal. Today 51 (1999) 319.
[3] T. Blasco, J.M. Lopez-Nieto, Oxidative dyhydrogenation of short chain alkanes on supported vanadium oxide catalysts, Appl. Catal. A. 157 (1997) 117.
[4] M.D. Argyle, K. Chen, A.T. Bell, E. Iglesia, Effect of catalyst structure on oxidative dehydrogenation of ethane and propene on alumina-supported vanadia, J. Catal. 208 (2002) 139.
[5] E.M. Thorsteinson, T.P. Wilson, F.G. Young, P.H. Kasai, The oxidative dehydrogenation of ethane over catalysts containing mixed oxides of molybdenum and vanadium, J. Catal. 52 (1978) 116.
[6] Y. Liu, P. Cong, R.D. Doolen, S. Guan, V. Markov, L. Woo, S. Zeyb, U. Dingerdissen, Discovery from combinatorial heterogeneous catalysis. A new class of catalyst for ethane oxidative dehydrogenation at low temperatures, Appl. Catal. A. 254 (2003) 59.
[7] E. Heracleous, A.F. Lee, I.A. Vasalos, A.A. Lemonidou, Surface properties and reactivity of Al_2O_3-supported MoO3 catalysts in ethane oxidative dehydrogenation, Catal. Lett. 88 (2003) 47.
[8] E. Heracleous, A.A. Lemonidou, Ni–Nb–O mixed oxides as highly active and selective catalysts for ethene production via ethane oxidative dehydrogenation. Part I: Characterization and catalytic performance, J. Catal. 237 (2006) 162.
[9] E. Heracleous, A.A. Lemonidou, Ni–Nb–O mixed oxides as highly active and selective catalysts for ethene production via ethane oxidative dehydrogenation. Part II: Mechanistic aspects and kinetic modelling, J. Catal. 237 (2006) 175.
[10] P. Arpentinier, F. Cavani, F. Trifiro, The Technology of Catalytic Oxidations, Technip, Paris, France, 2001.
[11] L.M. Rose, Chemical Reactor Design in Practice, Elsevier Scientific Pub. Co, New York, USA, 1981.
[12] G. Eigenberger, Fixed-bed reactors Ullmann's Encyclopedia of Industrial Chemistry, B4, VCH Publishers, Weinheim, Germany, 1992.
[13] N. Steinfeldt, N. Dropka, D. Wolf, M. Baerns, Application of multichannel microreactors for studying heterogeneous catalysed gas phase reactions, Trans. IChemE 81 (2003) 735.
[14] A.N. Zagoruiko, Simulation of selective reactions' performance in transient regimes with periodical separate feeding of reagents: Case study: Propane oxidative dehydrogenation in adiabatic V-Ti catalyst bed, Chem. Eng. J. 134 (2007) 117.
[15] A. Beretta, E. Ranzi, P. Forzatti, Oxidative dehydrogenation of light paraffins in novel short contact time reactors. Experimental and theoretical investigation, Chem. Eng. Sci. 56 (2001) 779.
[16] G.F. Froment, K.B. Bischoff, Chemical Reactor Analysis and Design, Wiley, Toronto, Canada, 1990.
[17] A. Marsella, P. Fatutto, D. Carmello, Catalyst and oxychlorination process using it, United States Patent 6465701, USA (2002).

[18] P.H. Calderbank, L.A. Pogorski, Heat transfer in packed beds, Trans. Inst. Chem. Eng. 35 (1957) 195.

[19] D.Q. Kern, Process Heat Transfer, McGraw-Hill, New York, USA, 1950.

[20] G.B. Marin, F. Kapteijn, A.E. van Diepen, J.A. Moulijn, Catalytic reaction and reactor engineering, in: E.G. Derouane, F. Lemos, A. Corma, F.R. Ribeiro (Eds.), Combinatorial Catalysis and High Throughput Catalyst Design and Testing, Kluwer Academic Publishers, Dordrecht, 2000.

[21] K.R. Westerterp, K.J. Ptasinski, Safe design of cooled tubular reactors for exothermic, multiple reactions: parallel reactions, Chem. Eng. Sci. 39 (2) (1984) 245.

[22] F. Cavani, N. Ballarini, A. Cericola, Oxidative dehydrogenation of ethane and propane: How far from commercial implementation? Catal. Today 127 (2007) 113.

[23] F.A. Al-Sherehy, A.M. Adris, M.A. Solimans, R. Hughest, Avoidance of flammability and temperature runaway during oxidative dehydrogenation using a distributed feed, Chem. Eng. Sci. 53 (1998) 3965.

[24] A.L.Y. Tonkovich, J.L. Zilka, D.M. Jiménez, G.L. Roberts, J.L. Cox, Inorganic membrane reactors for the oxidative coupling of methane, Chem. Eng. Sci. 51 (1996) 789.

[25] C. Téllez, M. Menéndez, J. Santamaría, Oxidative dehydrogenation of butane using membrane reactors, AIChE J. 43 (1997) 777.

[26] D. Achchieva, M. Peglow, S. Heinrich, L. Mörl, T. Wolff, F. Klose, Oxidative dehydrogenation of ethane in a fluidized bed membrane reactor, Appl. Catal. A 296 (2005) 176.